Configuration Optimization for Multiple Nonholonomic Mobile Manipulators with Holonomic Interaction

Chin Pei Tang

Abstract— **This paper presents an analytical method for quantitative performance analysis and configuration optimization for the cooperation of multiple nonholonomic mobile manipulators to transport a common object. The major challenge of such cooperation comes from the requirement of tight physical interactions between the robotic agents through a payload. The cooperation as a mobile constrained articulation system that takes into account the nonholonomic constraints due to the wheels together with the holonomic constraints due to the physical interactions are modeled and analyzed. Performance of several representative scenarios with varying actuation arrangements are then quantified in terms of manipulability measure. Subsequently, the measure is utilized to determine the optimal configuration of the cooperation permitting the payload transported in a near omnidirectional manner.**

I. Introduction

In the biological world, armies of ants leverage their collective strength to move large food pieces that would be impossible by a single ant. Biologists who study animal aggregations have also observed the remarkable group-level cooperative achievement of tasks in the nature. Hence, the very natural question that one would ask is whether or not such behaviors can be implemented in the robotics context to improve performance. Indeed, there has been increasing interest in deploying cooperative robotic system when certain tasks are either too complex to be performed by a single robot - such as carrying, transporting and manipulating a huge container - or when there are distinct benefits in terms of robustness, reliability and cost efficiency that accrue by deploying many simple cooperative robotic modules.

In this paper, the case where mobile robotic agents in the form of nonholonomic mobile manipulators [Fig. 1(a)] [1] to form a cooperative system when a common object is placed at the end-effectors of the multiple such modules [Fig. 1(b)] is considered. Such cooperation can help human in cooperatively transporting and manipulating a large payload either physically [2] or remotely [3]. The challenge then comes from the *physical* interaction between the multiple robots that can significantly affect the overall cooperation performance. Specifically, when a payload is placed at the end-effectors of the modules, holonomic (position) level constraints formed, which imposes more stringent constraints than those encountered in the popular research efforts that focus on multi-robot swarming or consensus [4]. The problem becomes more challenging when each module possesses multiple disc wheels that are subjected to nonholonomic constraints, which restrict the mobility of the cooperative system when they are tightly coupled together. In addition, the modularity also creates challenges by way of increased choice of means to accomplish given tasks. Hence, it is very important to synergize the modeling and design analysis for such systems to arrive at novel embodiments that provide new levels of robotic mobility and manipulability that would not otherwise be possible.

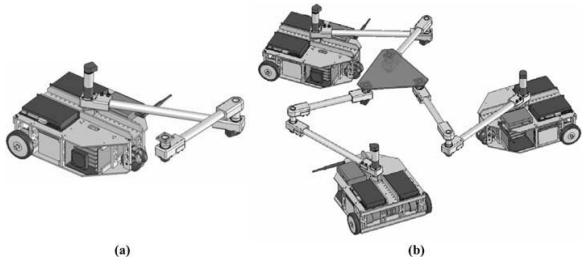

Fig. 1. (a) Representative nonholonomic wheeled mobile manipulator module, and (b) the cooperative system.

Evaluation and optimization of the quality of robotic system design rely heavily on the defined performance measures. Performance measures for a single robotic system are very well developed based on the Jacobian analysis. However, the extension of performance measures for multi-robot system is limited. Balch [5] developed a quantity called the social entropy to provide a quantitative evaluation of diversity of the robots in team. Energy based measures [6] developed using left-invariant Riemannian metrics [7] are used to characterize the aggregate kinetic energy of a formation, thus provide a framework to determine the optimal layout for formation-based operation. However, the importance in this paper is in the cooperative motion or force transmission capability due to the interaction between multiple end-effectors. Building from Yoshikawa's measure of manipulability [8] for the open serial chain case, there is a large variety of formulations for use in different applications [9]. The use of Singular Value Decomposition (SVD) of the Jacobian matrix offers further mathematical and geometrical insight of the manipulability characteristics of a robotic system [10]. However, efforts for characterizing the manipulability of constrained system tend to be more difficult [11], [12]. Such systems possesses multiple closed kinematic loops, and often offer diverse joint actuation schemes that can significantly affect the manipulability.

This work was supported in part by NSF CAREER Award Grant IIS-0347653 and UT Dallas Research Fund. The colored version of the paper can be found on IEEE Xplore.

C. P. Tang is currently with Erik Jonsson School of Engineering and Computer Science, University of Texas at Dallas, Richardson, TX 75080, USA. email: chinpei@ieee.org

The focus of this paper is the development of an integrated quantitative performance analysis and optimization scheme for a more challenging mobile cooperative system. In the presented approach, the cooperative system is analyzed within a constrained articulated mechanical system framework in the kinematic setting while taking into account the nonholonomic/holonomic constraints and different joint-actuation schemes within the system. Note that the analysis can be conveniently extended to different number of modules or with different number of joints. Manipulability measure in the form of isotropy index is them utilized to quantitatively analyze the cooperative system level performance with representative case studies. Finally, optimal configurations of such cooperative system permitting the payload transported to achieve near isotropic maneuver are then determined over two preferred actuated schemes.

II. Cooperation Model

In developing this model, the formulation from [12] is extended. the payload is treated as a common reference member of Type 0 simple-closed-chain system [13] and the various mobile manipulator modules as the serial-chain legs. For this paper, it is assumed that a rigid connection is formed between the payload and the end-effector, i.e. all mobility at the contact is localized within the attaching serial-chain. The cooperative system Jacobian matrix is shown to be formulated in a modular way so that it can handle arbitrary number of modules. The Jacobian matrix of each module is modeled by using the screw theoretic-based approach [14]. While the framework can be analyzed in a coordinate-free manner, in this paper, the generalized coordinates are implemented for convenience in analysis.

A. Cooperative System Model

Let the complete set of configuration variables of the constrained mechanical system be described by a vector of generalized position η, and the vector of the generalized velocities is $\dot{\eta}$. The (forward) kinematic model of the closed-loop constrained system at the velocity level can generally be written as:

$$J_T(\eta)\dot{\eta} = t^E \tag{1}$$

subject to the general constraints (at the velocity level) of:

$$J_C(\eta)\dot{\eta} = 0 \tag{2}$$

where $t^E = [\omega_z, v_x, v_y]^T$ is the payload (end-effector) planar twist[1] created at the payload frame $\{E\}$, ω_z is the angular velocity about the z-axis, v_x and v_y are respectively the x- and y-translational velocities. Such twist is the body-fixed twist that corresponds to the motion of the moving frame $\{E\}$ with respect to the global frame $\{F\}$ (as expressed in the moving frame $\{E\}$). Within a closed-loop system, not all the joints in the system need to be actuated. Hence, the generalized velocity vector can be partitioned into the active ($\dot{\eta}_a$) and passive ($\dot{\eta}_p$) components as $\dot{\eta}^T = [\dot{\eta}_a^T, \dot{\eta}_p^T]$. Jacobian matrices J_T and J_C can then be partitioned accordingly, permitting Eqs. (1) and (2) to be rewritten as:

$$J_{T_a}\dot{\eta}_a + J_{T_p}\dot{\eta}_p = t^E \tag{3}$$

$$J_{C_a}\dot{\eta}_a + J_{C_p}\dot{\eta}_p = 0 \tag{4}$$

Solving Eqs. (3) and (4), the closed-form solution that maps the actuation $\dot{\eta}_a$ to the task velocity t^E can then be determined as [12]:

$$t^E = \bar{J}_T\dot{\eta}_a + J_{T_p}\tilde{J}_{C_p}\xi \tag{5}$$

where

$$\bar{J}_T = J_{T_a} - J_{T_p}J_{C_p}^{+}J_{C_a} \tag{6}$$

where the superscript $^+$ denotes the Moore-Penrose inverse of the matrix, and ξ is any arbitrary vectors parameterizing the nullspace of J_{C_p}, and $\tilde{J}_{C_p}$ is the right annihilator of J_{C_p}, i.e. $J_{C_p}\tilde{J}_{C_p} = 0$.

B. Construction of Cooperative System Jacobian Matrix

If the cooperative system has N modules and labeled $I, II, \cdots, N$, and there are m active and n passive joints[2] in each module, and assume that all the modules are homogeneous[3], then the configuration of the cooperative system can be completely described by $N(m+n)$ generalized coordinates. The generalized velocities can then be partitioned into:

$$\begin{aligned}\dot{\eta}_a^T &= \begin{bmatrix} \{\dot{\eta}_a^I\}^T & \cdots & \{\dot{\eta}_a^N\}^T \end{bmatrix} \\ \dot{\eta}_p^T &= \begin{bmatrix} \{\dot{\eta}_p^I\}^T & \cdots & \{\dot{\eta}_p^N\}^T \end{bmatrix}\end{aligned} \tag{7}$$

For the forward kinematic, any of the module in the system can be picked as the "leader" and expressed by Eq. (3). The contributions by other modules can be set to 0. For instance, if Module I is designated as the "leader", J_{T_a} and J_{T_p} can then be determined as:

$$\begin{aligned}J_{T_a} &= \begin{bmatrix} J_a^I & \mathbf{0}_{3\times m} & \cdots & \mathbf{0}_{3\times m} \end{bmatrix} \\ J_{T_p} &= \begin{bmatrix} J_p^I & \mathbf{0}_{3\times m} & \cdots & \mathbf{0}_{3\times m} \end{bmatrix}\end{aligned} \tag{8}$$

Note that the size of J_a^k and J_p^k are $3\times m$ and $3\times n$, respectively. For the constraints, there are two ways to formulate J_{C_a} and J_{C_p}, which can be identified in Chiacchio et al. [15]. The following form based on the loop closure equation is determined as:

$$\begin{aligned}J_{C_a} &= \begin{bmatrix} J_a^I & -J_a^{II} & \mathbf{0}_{3\times m} & & \cdots & \mathbf{0}_{3\times m} \\ J_a^I & \mathbf{0}_{3\times m} & -J_a^{III} & \cdots & \mathbf{0}_{3\times m} & \mathbf{0}_{3\times m} \\ \vdots & \vdots & \vdots & \ddots & \vdots & \vdots \\ J_a^I & \mathbf{0}_{3\times m} & \mathbf{0}_{3\times m} & \cdots & \mathbf{0}_{3\times m} & -J_a^N \end{bmatrix} \\ J_{C_p} &= \begin{bmatrix} J_p^I & -J_p^{II} & \mathbf{0}_{3\times m} & & \cdots & \mathbf{0}_{3\times m} \\ J_p^I & \mathbf{0}_{3\times m} & -J_p^{III} & \cdots & \mathbf{0}_{3\times m} & \mathbf{0}_{3\times m} \\ \vdots & \vdots & \vdots & \ddots & \vdots & \vdots \\ J_p^I & \mathbf{0}_{3\times m} & \mathbf{0}_{3\times m} & \cdots & \mathbf{0}_{3\times m} & -J_p^N \end{bmatrix}\end{aligned} \tag{9}$$

[1] Twist can generally be interpreted as the velocity of the system in a vectorial form. It provides a convenient general velocity analysis using screw theory and can be generalized to the 3-dimensional analysis easily.

[2] In this paper, joints are loosely defined as the single DOF "manipulation" variable.

[3] The analysis is, of course generalizable to the heterogeneous case. Without too much elaboration, and without the lost of generality, the analysis is restricted to only homogeneous cases in this paper.

C. Isotropy Index

After formulating the solution of the system Jacobian matrix, the manipulability-based performance measure is developed, so that the configuration of the cooperative system can be optimized. The system Jacobian matrix $\bar{J}_T$ maps the active joint rates into both the translational and orientational task-space velocities. In this paper, the translational mapping is focused - the sub-matrix of the second and the third rows of $\bar{J}_T$, which is denoted $\bar{J}_{T,trans}$. The SVD of this matrix can now be used to examine the manipulability characteristics and its interpretation in the context of the manipulability ellipsoid geometry. In this paper, the *isotropy index* is adopted and defined as:

$$\Gamma = \frac{\sigma_{min}}{\sigma_{max}} \tag{10}$$

which is the measure-of-choice to characterize the performance of the cooperative system. Here, σ_{min} and σ_{max} are respectively the minimum and the maximum singular values of matrix $\bar{J}_{T,trans}$.

III. Individual Module Model

Following Murray *at. al.* [16], the homogeneous matrix is used to represent the configurations of the system. The analysis is specialized for nonholonomic mobile manipulators formed by three revolute (R) joints [see Fig. 2]. For the kth module, the frame $\{M^k\}$ is rigidly attached to the wheeled mobile base (MB), such that the y-axis is directed to the nonholonomic constraint[4], and the frames $\{A^k\}$, $\{B^k\}$ and $\{E^k\}$ are assigned in a standard convention. For generality, the (body-fixed) payload frame $\{E\}$ is considered to attached to the payload is offset with respect to the end-effector frame $\{E^k\}$ by a constant angle δ_k. The configuration of the manipulator can be parameterized by the three relative angles, θ_1, θ_2 and θ_3, with the link lengths L_1, L_2 and L_3. The module Jacobian matrix is constructed by determining the twist contribution by each DOF available in the system and the twist vectors are assembled in columns. All the twist vectors are finally expressed in the payload frame $\{E\}$.

A. Treatment of Nonholonomic Constraint

In this section, the treatment of the nonholonomic constraint of the mobile base (MB) is described. The configuration of the mobile base can be written as the homogeneous matrix of:

$$g_{fm}(x_M, y_M, \phi) = \begin{bmatrix} \cos\phi & -\sin\phi & x_M \\ \sin\phi & \cos\phi & y_M \\ 0 & 0 & 1 \end{bmatrix} \tag{11}$$

Computing the body-fixed twist (in frame $\{M\}$) of the MB by:

$$V^M_{fm} = g^{-1}_{fm}\dot{g}_{fm} = \begin{bmatrix} 0 & -\dot{\phi} & \dot{x}_M\cos\phi + \dot{y}_M\sin\phi \\ \dot{\phi} & 0 & -\dot{x}_M\sin\phi + \dot{y}_M\cos\phi \\ 0 & 0 & 0 \end{bmatrix} \tag{12}$$

[4]The rationale of this choice is shown in [14].

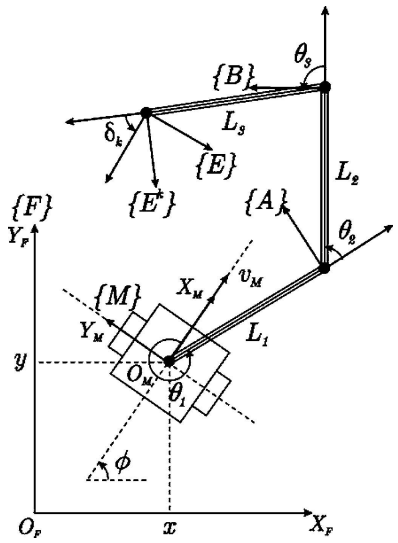

Fig. 2. Kinematic model of individual wheeled mobile manipulator module.

Realizing that the nonholonomic constraint is in the y-direction of the MB:

$$-\dot{x}_m\sin\phi + \dot{y}_m\cos\phi = 0 \tag{13}$$

and, assuming that the wheels are rolling without slipping, the forward velocity of the MB is:

$$\dot{x}_m\cos\phi + \dot{y}_m\sin\phi = v_M \tag{14}$$

Eq. (12) then becomes:

$$V^M_{fm} = \begin{bmatrix} 0 & -\dot{\phi} & v_M \\ \dot{\phi} & 0 & 0 \\ 0 & 0 & 0 \end{bmatrix} \tag{15}$$

Hence, using the $\vee$ operator to extract the twist vectors of the system, the 2 DOF twists for the MB can be formed and expressed in the $\{M\}$ frame as:

$$t^M_{\dot{\phi}} = \begin{bmatrix} 1 \\ 0 \\ 0 \end{bmatrix}, t^M_{v_M} = \begin{bmatrix} 0 \\ 0 \\ 1 \end{bmatrix}$$

Note that these twist vectors are currently expressed in the MB frame $\{M\}$, so it needs to be expressed in frame $\{E\}$ by adjoint transformation. All the other twists (with respect to the payload frame $\{E\}$) contributed by each DOF within the module can then be determined in the standard manner

[14], and they are listed in the following:

$$t^E_{\dot{\phi}} = \begin{bmatrix} 1 \\ -L_1\sin(\delta_k-\theta_2-\theta_3)-L_2\sin(\delta_k-\theta_3)-L_3\sin\delta_k \\ L_1\cos(\delta_k-\theta_2-\theta_3)+L_2\cos(\delta_k-\theta_3)+L_3\cos\delta_k \end{bmatrix},$$

$$t^E_{v_M} = \begin{bmatrix} 0 \\ \cos(\delta_k-\theta_1-\theta_2-\theta_3) \\ \sin(\delta_k-\theta_1-\theta_2-\theta_3) \end{bmatrix},$$

$$t^E_{\dot{\theta}_1} = \begin{bmatrix} 1 \\ -L_1\sin(\delta_k-\theta_2-\theta_3)-L_2\sin(\delta_k-\theta_3)-L_3\sin\delta_k \\ L_1\cos(\delta_k-\theta_2-\theta_3)+L_2\cos(\delta_k-\theta_3)+L_3\cos\delta_k \end{bmatrix},$$

$$t^E_{\dot{\theta}_2} = \begin{bmatrix} 1 \\ -L_2\sin(\delta_k-\theta_3)-L_3\sin\delta_k \\ L_2\cos(\delta_k-\theta_3)+L_3\cos\delta_k \end{bmatrix}, t^E_{\dot{\theta}_3} = \begin{bmatrix} 1 \\ -L_3\sin\delta_k \\ L_3\cos\delta_k \end{bmatrix}$$

where k represents the k module. Finally, the module Jacobian can be determined as:

$$\underbrace{\begin{bmatrix} t^E_{\dot{\phi}} & t^E_{v_M} & t^E_{\dot{\theta}_1} & t^E_{\dot{\theta}_2} & t^E_{\dot{\theta}_3} \end{bmatrix}}_{J_T} \begin{bmatrix} \dot{\phi} \\ v_M \\ \dot{\theta}_1 \\ \dot{\theta}_2 \\ \dot{\theta}_3 \end{bmatrix} = t^E \qquad (16)$$

which is in the form of Eq. (1). Finally, the active and passive Jacobian components for each module can then be selected/arranged based on the following manner:

$$\begin{bmatrix} J^k_a & J^k_p \end{bmatrix} \begin{bmatrix} \dot{\eta}^k_a \\ \dot{\eta}^k_p \end{bmatrix} = t^E \qquad (17)$$

IV. Representative Case Studies

Consider the case of three mobile manipulators coming together in a formation to cooperatively transport a common payload. The study of three-module case permits to provide linkage to some existing literature, such as the traditional stationary 3-RRR planar parallel mechanisms [17]. The individual modules are numbered I, II and III, as depicted in Fig. 3. Ri^k denotes the revolute joints and MB^k denotes the mobile bases, where $i = 1,2,3$ and $k = I, II, III$[5]. When an object is placed at the end-effectors of the mobile manipulator modules, it effectively creates a mobile 3-RRR planar parallel mechanism. Instantaneously, each MB is considered to form a 2-DOF nonholonomic "joint" while each revolute joint possesses 1 DOF. Further design limitations are imposed, such as requiring identical mobile modules, i.e. the mobile bases have the same size and the manipulators have the same link lengths, and the symmetry of actuation within the contributing sub-chains.

There are 27 possible permutations based on whether MB, R1 and R2 are chosen to be locked, passive or made active. In this paper, 4 representative cases were identified for studied and listed in Fig. 5. For this study, the MBs are located at the vertices of an equilateral triangle of side $4m$, with the payload taking the form of another equilateral triangle of sides $1.732m$ as shown in Fig. 4. The payload frame $\{E\}$ is

[5]Note that the formulation can be extended to increasing numbers of modules as well as take into account the various selections of actuator locations within the system.

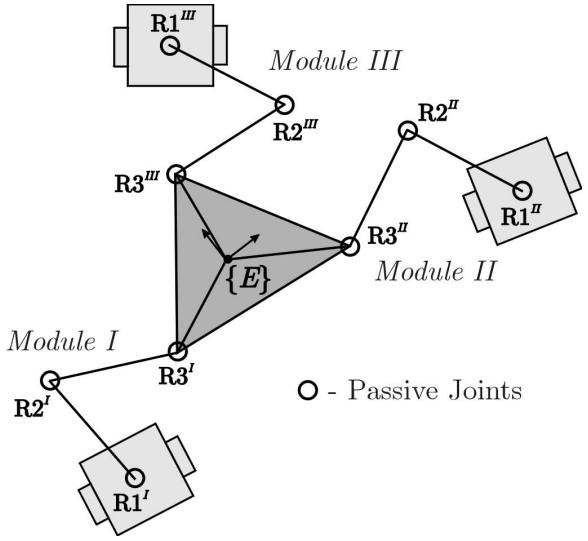

Fig. 3. Notation and labeling convention of cooperating 3 mobile manipulators

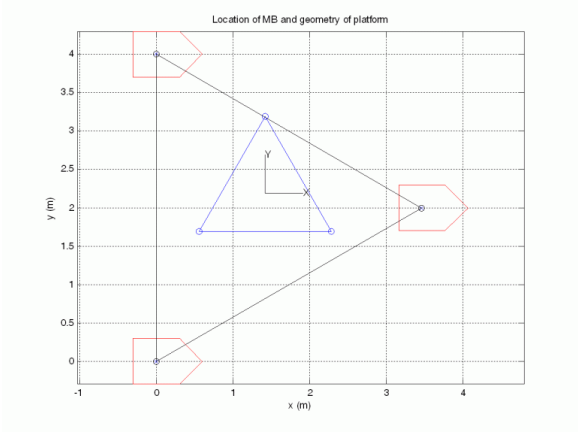

Fig. 4. Location of the mobile bases and the geometry of the platform

assumed to be located at the centroid of the payload-triangle with an orientation $\phi_E = 0^\circ$. The important dimensions are shown in Table I. However, the mechanism has 8 working modes with different elbow configurations - here only elbow down configurations are considered. The isotropy indexes bounded between 0 and 1 are computed using the formulation over the entire feasible workspace, where all the results are shown in the form of pseudo-color plots in Fig. 5 for all the 4 actuation schemes. It is interesting to note that the results for the MBs are locked are nothing more than the traditional fixed-based planar parallel manipulator. For instance, Case I represents the isotropy index of an 3-$\underline{\text{R}}$RR[6], while Case II represents the result for an 3-R$\underline{\text{R}}$R. Hence, the methods further generalize to account for these cases. Case III and IV now represent the cases when the bases are allowed to move in a nonholonomic manner, which will form the next optimization study.

[6]The underline under the first "R" indicates that the first joint of each manipulator chain is actuated.

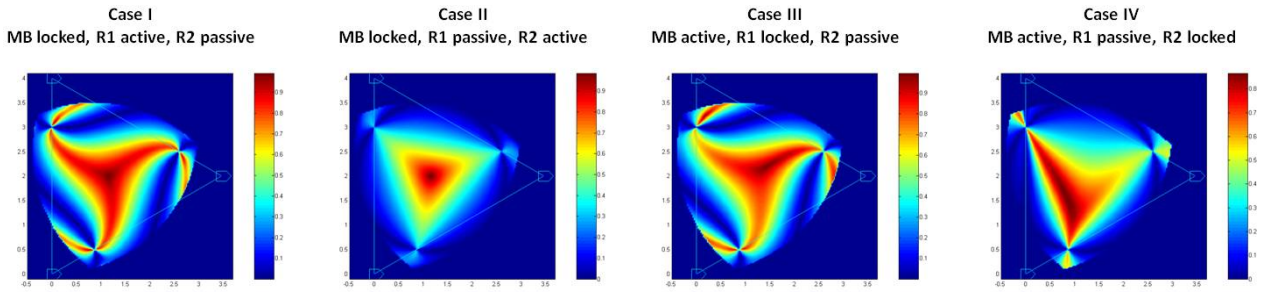

Fig. 5. Pseudo-color plots of the isotropy index of different cases of cooperative systems

TABLE I
DETAILED STUDY PARAMETERS

Link Lengths	$L_1^k = L_2^k = 1.5m, L_3^k = 1.0m$
Base Positions	$(0,0),(3.462,2),(0,4)$, for I,II,III
Offset Angles	$\delta^I = 330°, \delta^{II} = 210°, \delta^{III} = 90°$

V. CONFIGURATION OPTIMIZATION

The optimal configuration of the formation of the cooperative system can be determined to achieve near isotropic (omni-directional) maneuver using the isotropic index. The study is similar to [18], but the presented approach can effectively compare different actuation schemes. In the case under consideration, the configuration that has the highest isotropy index corresponds to the most isotropic configuration. From the plots in all the case studies presented in previous sections, it can be seen that the isotropy index behave quite well within the workspace (unimodal and smooth). The optimization problem can then be setup as:

$$\min_{\eta} -\Gamma(\eta) \tag{18}$$

subject to: closed-loop kinematic constraints, where $\eta^T = [\theta^I, \theta^{II}, \theta^{III}]$, $\theta^k = [\theta_1^k, \theta_2^k, \theta_3^k]$, $k = I,II,III$. The structural parameters, including the link lengths, location of the MBs, the platform offset angles, and the elbow configurations are set to be constants in this study. In this case, the inverse kinematic problem can be solved explicitly in terms of the payload frame positions, which also at the same time satisfy the closed-loop kinematic constraints, so the optimization can be restated as an unconstrained optimization problem of:

$$\min_{(x_E,y_E)} -\Gamma((x_E,y_E)) \tag{19}$$

where the new design variable is the payload frame position (x_E,y_E). The optimal configuration can then be determined for Case III and IV by employing the MATLAB `fminunc` function. The complete configuration of the system can then be solved by inverse kinematics.

Case III: MB actuated and R1 locked: In the case of MB actuated and R1 locked in Case III, the optimal configuration is found to be at the payload frame position of $(x_E,y_E) = (1.42m, 2.19m)$ and the isotropy index at the configuration is $\Gamma^* = 1.000$. The corresponding configuration is determined as:

$$\theta^I = [0.32, 1.87, -7.95] = [18.2°, 107.4°, 264.5°]$$
$$\theta^{II} = [2.23, 2.31, -8.22] = [128.8°, 132.1°, 249.1°]$$
$$\theta^{III} = [4.77, -4.30, -2.05] = [273.3°, 113.9°, 242.8°]$$

The configuration is also plotted in Fig. 6(a).

Case IV: MB actuated and R2 locked: In the case of MB actuated and R2 locked in Case IV, the optimal configuration is found to be at the payload frame position of $(x_E,y_E) = (0.87m, 1.50m)$ and the isotropy index at this configuration is $\Gamma^* = 0.866$. The corresponding joint angles are then determined as:

$$\theta^I = [0.34, 2.46, -8.56] = [19.5°, 141.1°, 229.5°]$$
$$\theta^{II} = [2.82, 1.68, -8.17] = [161.8°, 96.4°, 251.8°]$$
$$\theta^{III} = [4.28, 1.91, -7.76] = [245.3°, 109.5°, 275.3°]$$

The configuration is also plotted in Fig. 6(b). By comparing the above two results, it may be concluded that locking joints R1 can perform better in terms of manipulability since the isotropy index that can achieve in this case is 1.000, while the isotropy index for locking joints R2 is 0.866.

VI. CONCLUSION

In this paper, the formulation of the system-level isotropy index of the entire cooperating system is examined as a measure of overall system performance for different actuation schemes. In particular, the cooperating system is treated as a Type 0 simple constrained mechanical system. This work takes the nonholonomic constraints, kinematic loop-closure constraints and mixtures of active, locked and passive joints into account explicitly into to full kinematic model. System-level performance measures are developed for the overall cooperating system, in terms of the system-level Jacobian matrix. In this paper, it is recognized that the cooperating system performance depends critically upon the dimension, configuration and actuation and focused on the role of the joint-actuation-schemes within the system. The designer has the choice of selectively actuating, locking or rending passive the various joints within the system - all of which affect the system performance. The case studies, using the mobile

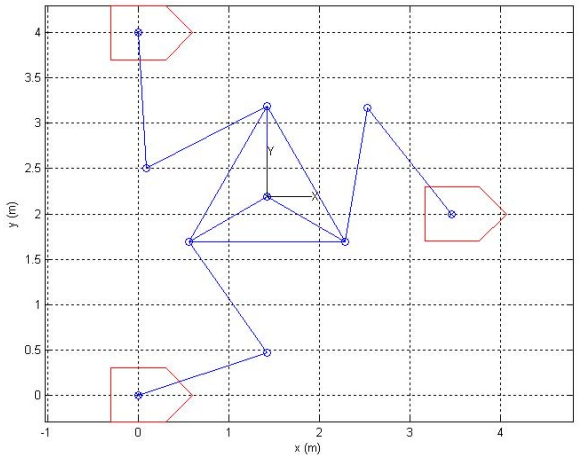

(a) Case III: MB actuated and R1 locked

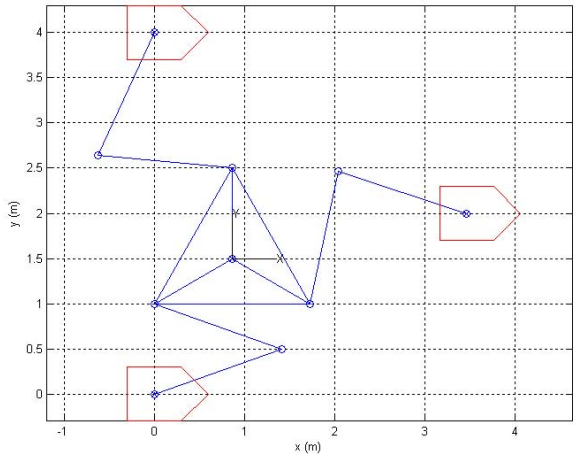

(b) Case IV: MB actuated and R2 locked

Fig. 6. Optimal configuration

3-RRR planar manipulator configuration permitted to study the effect of different actuation schemes on the isotropy index surface. Finally, the performance measure is utilized to determine the optimal cooperative configuration permitting the payload transported to achieve near isotropic maneuver. It can be concluded that locking joint R1 is preferred configuration. Future work includes the force manipulability analysis of the system based on the dynamic characteristics of the payload.

VII. Acknowledgments

The author gratefully acknowledge the prior collaboration with V. N. Krovi for this work. The author also gratefully acknowledge the prior partial funding from NSF CAREER Grant IIS-0347653, and UT Dallas research fund from M. W. Spong for this continuing effort.

References

[1] G. D. White, R. M. Bhatt, C. P. Tang, and V. N. Krovi, "Experimental evaluation of dynamic redundancy resolution in a nonholonomic wheeled mobile manipulator," *IEEE/ASME Transactions on Mechatronics*, vol. 14, no. 3, pp. 349–357, June 2009.

[2] Y. Hirata, Y. Kume, Z.-D. Wang, and K. Kosuge, "Handling of a single object by multiple mobile robots based on caster-like dynamics," in *Proceedings of the 2008 IEEE International Conference on Robotics and Automation*, Pasadena, California, USA, 2008, pp. 2215–2216.

[3] Dongjun Lee, Oscar Martinez-Palafox, and Mark W. Spong, "Bilateral teleoperation of multiple cooperative robots over delayed communication networks: Application," in *Proceedings of the 2005 IEEE International Conference on Robotics and Automation*, Barcelona, Spain, 2005, pp. 368–373.

[4] Dongjun Lee and Mark W. Spong, "Stable flocking of multiple inertial agents on balanced graphs," *IEEE Transactions on Automatic Control*, vol. 52, no. 8, pp. 1469–1475, August 2007.

[5] T. Balch, "Hierarchic social entropy: An information theoretic measure of robot group diversity," *Autonomous robots, Kluwer Academic Publishers, The Netherlands*, vol. 8, pp. 209–237, 2000.

[6] R. M. Bhatt, C. P. Tang, and V. Krovi, "Geometric motion planning and formation optimization for a fleet of nonholonomic wheeled mobile robots," in *Proc. 2004 IEEE International Conference of Robotics and Automation*, New Orleans, LA, USA, 2004.

[7] M. Zefran, V. Kumar, and C. B. Croke, "On the generation of smooth three-dimensional rigid body motions," *IEEE Transactions on Robotics and Automation*, vol. 14, no. 4, pp. 576–589, August 1998.

[8] T. Yoshikawa, "Manipulability of robotic mechanisms," *The International Journal of Robotics Research*, vol. 4, no. 2, pp. 3–9, 1985.

[9] Y. Yamamoto and X. Yun, "Unified analysis on mobility and manipulability of mobile manipulators," in *Proc. 1999 IEEE International Conference on Robotics and Automation*, Detroit, MI, USA, May 1999, pp. 1200–1206.

[10] Y. Nakamura, *Advanced robotics: Redundancy and optimization*, Addison-Wesley, 1991.

[11] A. Bicchi and D. Prattichizza, "Manipulability of cooperating robots with unactuated joints and closed-chain mechanisms," *IEEE Transactions on Robotics and Automation*, vol. 16, no. 4, pp. 336–345, 2000.

[12] J. T.-Y. Wen and L. S. Wilfinger, "Kinematic manipulability of general constrained rigid multibody systems," *IEEE Transactions on Robotics and Automation*, vol. 15, no. 3, pp. 558–567, 1999.

[13] K. W. Lilly, *Efficient dynamic simulation of robotic mechanisms*, Kluwer Academic Publishers, Norwell, MA, USA, 1993.

[14] C. P. Tang, R. M. Bhatt, M. Abou-Samah, and V. N. Krovi, "Screw-theoretic analysis framework for payload transport by mobile manipulator collectives," *IEEE/ASME Transactions on Mechatronics*, vol. 11, no. 2, pp. 169–178, April 2006.

[15] L. Sciavicco P. Chiacchio, S. Chiaverini and B. Siciliano, "Global task space manipulability ellipsoids for multiple-arm system," *IEEE Transactions on Robotics and Automation*, vol. 7, no. 5, pp. 678–685, 1991.

[16] R. M. Murray, Z. Li, and S. S. Sastry, *A Mathematical Introduction to Robotic Manipulation*, CRC Press, Boca Raton, FL, USA, 1994.

[17] I. A. Bonev, D. Zlatanov, and C. Gosselin, "Singularity analysis of 3-dof planar parallel mechanisms via screw theory," *ASME Journal of Mechanical Design*, vol. 125, pp. 573–581, 2003.

[18] T. B. Park, J. H. Lee, B.-J. Yi, W. K. Kim, B. J. You, and S.-R. Oh, "Optimal design and actuator sizing of redundantly actuated omni-directional mobile robots," in *Proc. 2002 IEEE International Conference on Robotics and Automation*, Washington DC, USA, 2002.